

# Mechanism of the Palladium-Catalyzed Metal–Carbon Bond Formation. Isolation of Oxidative Addition and Transmetalation Intermediates<sup>†</sup>

Paola Cianfriglia, Valentina Narducci, Claudio Lo Sterzo,\* and Egidio Viola

Centro CNR di Studio sui Meccanismi di Reazione, Dipartimento di Chimica,  
Università "La Sapienza", Piazzale Aldo Moro 5, I-00185 Roma, Italy

Gabriele Bocelli and Thomas A. Kodenkandath

Centro di Studio per la Strutturistica Diffraattometrica del CNR, Viale delle Scienze,  
I-43100 Parma, Italy

Received March 14, 1996<sup>®</sup>

To investigate the reaction mechanism of the Pd-catalyzed metal–carbon bond formation, the model compounds  $[\eta^5\text{-1-Ph}_2\text{P-2,4-Ph}_2\text{C}_5\text{H}_2](\text{CO})_3\text{MI}$  (M = Mo, **12**; M = W, **13**) have been prepared and their reactions studied under coupling conditions. Treatment of **12** and **13** with stoichiometric amounts of zerovalent palladium yields the complexes  $[\eta^5\text{-1-Ph}_2\text{P-2,4-Ph}_2\text{C}_5\text{H}_2](\text{CO})_3\text{MPd}(\text{PPh}_3)\text{I}$  (M = Mo, **16**; M = W, **17**) by oxidative addition of the M–I moieties on Pd<sup>0</sup>. Subsequent reaction of intermediates **16** and **17** with 4-nitro-1-[2-(tributylstannyl)ethynyl]benzene ( $\text{Bu}_3\text{SnC}\equiv\text{C}(\text{C}_6\text{H}_4)\text{p-NO}_2$ , **18**) leads to the formation of the transmetalation products  $[\eta^5\text{-1-Ph}_2\text{P-2,4-Ph}_2\text{C}_5\text{H}_2](\text{CO})_3\text{MPd}(\text{PPh}_3)\text{C}\equiv\text{C}(\text{C}_6\text{H}_4)\text{p-NO}_2$  (M = Mo, **19**; W, **20**), which have been isolated and characterized. Complexes **13** and **17** have been also characterized by X-ray analysis.

## Introduction

The paramount importance of palladium catalysis in transition metal-mediated organic synthesis has long been recognized and well-established. In particular, the coupling between organostannane and nucleophiles in the presence of palladium, i.e., the Stille conditions, represents one of the most efficient and useful applications.<sup>1</sup> In this respect, Farina has recently ascertained that now the great majority of transition metal-mediated cross-coupling reactions reported in the literature are performed by the Stille reaction.<sup>1d</sup> In this field, we have reported the unusual catalytic properties of palladium in the formation of metal–carbon bond.<sup>2</sup> The exploration of this new reaction has immediately revealed interesting perspectives for the preparation of organometallic structures. We reported the formation of a variety of mono and bis transition metal  $\sigma$ -acetylides complexes by coupling of transition metal halides and mono and bis trialkyltin acetylides<sup>3</sup> (Scheme 1). The

products are formed only in the presence of zerovalent palladium. These compounds are models and building blocks of highly ethynylated organometallic structures, a subject of relevant interest in material science.<sup>4</sup>

Because of our interest in the reaction mechanism of this special catalytic behavior of palladium, we decided to look for analogies with the mechanism of the palladium-catalyzed carbon–carbon coupling, which is outlined in Figure 1.<sup>1,5,6</sup> The catalytic cycle consists of (a) oxidative addition of the electrophile on zerovalent palladium, (b) transmetalation with an organotin compound, (c) *trans* to *cis* isomerization of R ligands, and (d) reductive elimination to yield the coupled product.

It must be noted that, although single intermediates and segments of this picture have been independently studied and characterized in a number of cases,<sup>1d,7</sup> no example has ever been reported of a single reaction that has allowed the mapping of the overall catalytic cycle. Moreover, a number of recent reports reveal that a more

<sup>†</sup> C. Lo Sterzo dedicates this work to the memory of his beloved brother, Edoardo Lo Sterzo, deceased on April 23, 1995.

\* Address correspondence to this author. E-mail: losterzo@netmgr.ced.rm.cnr.it.

<sup>®</sup> Abstract published in *Advance ACS Abstracts*, November 1, 1996.

(1) (a) Heck, R. F. *Palladium in Organic Synthesis*; Academic Press: New York, 1985. (b) Stille, J. K. *Pure Appl. Chem.* **1985**, *56*, 1771. (c) Stille, J. K. *Angew. Chem., Int. Ed. Engl.* **1986**, *25*, 508. (d) Farina, V.; Krishnan, B.; Marshall, D. R.; Roth, G. P. *J. Org. Chem.* **1993**, *58*, 5434. (e) Schlosser, M., Ed. *Organometallics in Synthesis*; John Wiley & Sons Ltd.: Chichester, England, 1994. (f) Collman, J. P.; Hegedus, L. S.; Norton, J. R.; Finke, R. G. *Principles and Applications of Organotransition Metal Chemistry*; University Science Books: Mill Valley, CA, 1987. (g) Saa', J. M.; Martorell, G.; Garcia-Raso, A. *J. Org. Chem.* **1992**, *57*, 678. (h) Mitchell, T. N. *Synthesis* **1992**, 803.

(2) (a) Lo Sterzo, C. *J. Chem. Soc., Dalton Trans.* **1992**, 1989. (b) Crescenzi, R. Tesi di Laurea, Università di Roma "La Sapienza", Roma, Italy, 1992.

(3) (a) Crescenzi, R.; Lo Sterzo, C. *Organometallics* **1992**, *11*, 4301 and references therein. (b) Viola, E.; Lo Sterzo, C.; Crescenzi, R.; Frachey, G. *J. Organomet. Chem.* **1995**, *493*, 55. (c) Viola, E.; Lo Sterzo, C.; Crescenzi, R.; Frachey, G. *J. Organomet. Chem.* **1995**, *493*, C9. (d) Trezzi, F.; Viola, E.; Lo Sterzo, C. *Organometallics*, in press.

(4) (a) Bruce D. W.; O'Hare D. *Inorganic Materials*; John Wiley & Sons: Chichester, England, 1992. (b) Sun, Y.; Taylor, N. J.; Carty, A. *J. Organometallics* **1992**, *11*, 4293. (c) Lichtenberger, D. L.; Renshaw, S. K.; Wong, A.; Tagge, C. *Organometallics* **1993**, *12*, 3522. (d) Beck, W.; Niemer, B.; Wieser, M. *Angew. Chem. Int. Ed. Engl.* **1993**, *32*, 923. (e) Lang, H. *Angew. Chem., Int. Ed. Engl.* **1994**, *33*, 547.

(5) Morita, D. K.; Stille, J. K.; Norton, J. R. *J. Am. Chem. Soc.* **1995**, *117*, 8576 and references therein.

(6) Pereyre, M.; Quintard, J.-P.; Rahm, A. *Tin in Organic Synthesis*; Butterworths & Co: London, England, 1987.

(7) (a) Brown, J. M.; Cooley, N. A. *Organometallics* **1990**, *9*, 353. (b) Amatore, C.; Jutand, A.; Suarez, A. *J. Am. Chem. Soc.* **1993**, *115*, 9531 and references therein. (c) Farina, V.; Krishnan, B. *J. Am. Chem. Soc.* **1991**, *113*, 9585. (d) Stang, P. J.; Kowalski, M. H.; Schiavelli, M. D.; Longford, D. *J. Am. Chem. Soc.* **1989**, *111*, 3347.

Scheme 1

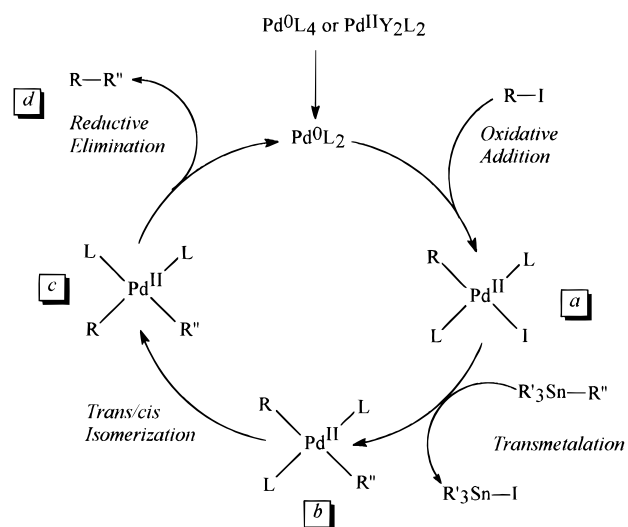
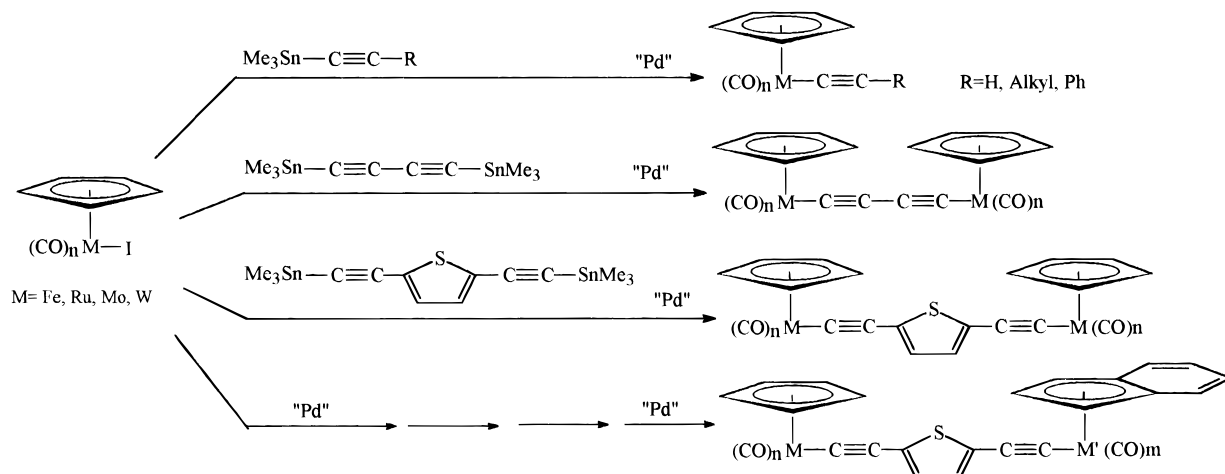
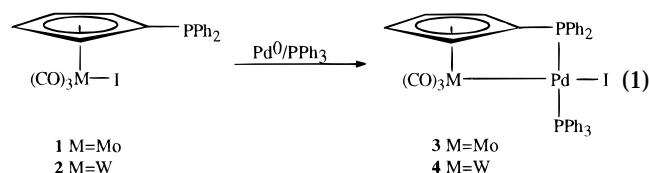


**Figure 1.** Mechanism of the palladium-catalyzed carbon-carbon coupling.

complicated mosaic underlies this simplified picture.<sup>5</sup> However, these new findings do not rule out this scheme that still remains a useful model to refer to, in order to explain key features of the cross-coupling of organotin compounds with organic electrophiles.

We then focused our attention on the isolation of intermediates from the reactions outlined in Scheme 1. Attempts to isolate the products that may be formed upon reacting stoichiometric amounts of simple cyclopentadienyl metal iodides  $(\eta^5\text{-C}_5\text{H}_5)\text{M}(\text{CO})_n\text{I}$  ( $\text{M} = \text{Fe}$ ,  $n = 2$ ;  $\text{M} = \text{Mo}$ ,  $n = 3$ ;  $\text{M} = \text{W}$ ,  $n = 3$ ) and zerovalent palladium were not successful.<sup>2b</sup> Therefore, we turned our attention to the (diphenylphosphino)cyclopentadienyl complexes **1** and **2** (eq 1), with the expectation that the dangling phosphine arm linked to Cp may serve as a trap for palladium after the insertion into the M–I moiety.<sup>8,9</sup> This was correct, and the M–Pd–I complexes



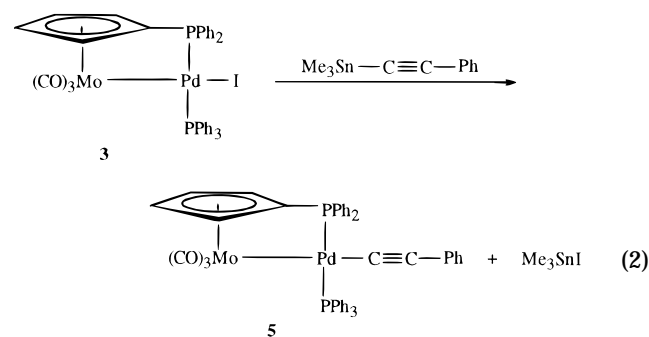
**3** and **4** were isolated and fully characterized.<sup>10</sup> This result showed the analogy between the first step of the

palladium-catalyzed *metal-carbon* coupling and the oxidative addition step in *carbon-carbon* coupling (intermediate **a** in Figure 1). Unfortunately, **3** and **4** were isolated in low yields, and crystals suitable for X-ray analysis could not be obtained.

In this article, we report some new examples of this reaction in which the system is tailored to allow the isolation of stable oxidative addition products M–Pd–I. These compounds have also been reacted further with stannylacetylides in order to study the subsequent step of the reaction mechanism.

## Results

The first attempt to elucidate further the mechanism of the *metal-carbon* bond formation was performed by reacting complexes **3** and **4** with trialkyltin acetylides  $\text{R}_3\text{SnC}\equiv\text{CPh}$  ( $\text{R} = \text{Me}$ ,  $\text{Bu}$ ) in DMF. Although starting materials were rapidly consumed, any attempts to isolate reaction products failed. However, observation by <sup>1</sup>H and <sup>31</sup>P NMR (Table 1) was consistent with the transmetalation reaction indicated in Eq 2. Upon the



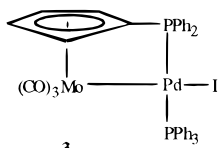
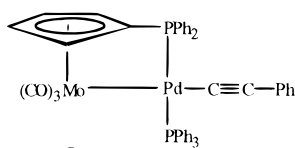
addition of 1 equiv of  $\text{Me}_3\text{SnC}\equiv\text{CPh}$  to a solution of **3** in  $\text{DMF-}d_7$ , the two quartets at 5.79 and 4.67 ppm relative to the  $\alpha, \alpha'$  and  $\beta, \beta'$  Cp ring slightly changed to 5.73 and 4.67 ppm, and two new sets of multiplets

(8) Baker, K. V.; Brown, J. M.; Cooley, N. A.; Huges, G. D.; Taylor, R. J. *J. Organomet. Chem.* **1989**, *370*, 397.

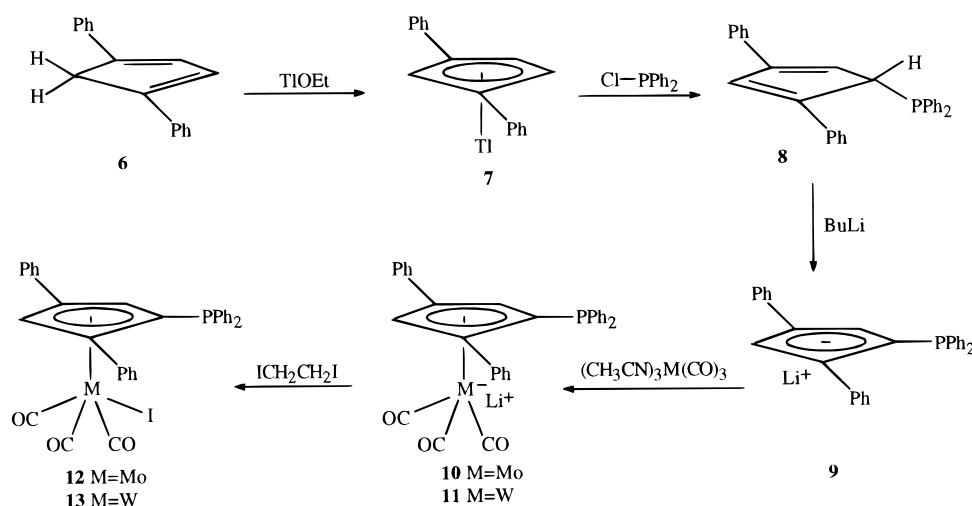
(9) (a) Bullock, R. M.; Casey, C. P. *Acc. Chem. Res.* **1987**, *20*, 167. Stille, J. K.; Smith, C.; Anderson, O. P.; Miller, M. M. *Organometallics* **1989**, *8*, 1040. (b) Brumas, B.; de Caro, D.; Dahan, F.; de Montauzon, D.; Poliblanco, R. *Organometallics* **1993**, *12*, 1503. (c) Ladipo, F. T.; Anderson, G. K.; Rath, N. P. *Organometallics*, **1994**, *13*, 4741.

(10) Spadoni, L.; Lo Sterzo, C.; Crescenzi, R.; Frachey, G. *Organometallics* **1995**, *14*, 3149.

**Table 1.**  $^1\text{H}$  and  $^{31}\text{P}$  NMR Data for Complexes **3** and **5**

	$^1\text{H}$ NMR <sup>a</sup>				$^{31}\text{P}$ NMR <sup>b</sup>
	Cp	PPh <sub>2</sub>	PPh <sub>3</sub>	-C≡C-Ph	
 <b>3</b>	5.79, q, 2H, $J = 2.0$ Hz ( $\alpha-\alpha'$ )	8.32–8.24, m, 4H ( <i>ortho</i> )	7.98–7.42, br, 6H ( <i>ortho</i> )		33.55, d, $J = 456$ Hz
	4.67, q, 2H, $J = 2.0$ Hz ( $\beta-\beta'$ )	7.23–7.60, m, 6H ( <i>meta, para</i> )	7.59–7.45, br, 9H ( <i>meta, para</i> )		17.00, d, $J = 456$ Hz
 <b>5</b>	5.73, q, 2H, $J = 2.0$ Hz ( $\alpha-\alpha'$ )	8.62–8.55, m, 4H ( <i>ortho</i> )	8.10–7.70, br, 6H ( <i>ortho</i> )	6.51–6.47, m, 2H ( <i>ortho</i> )	35.80, d, $J = 454$ Hz
	4.67, q, 2H, $J = 2.0$ Hz ( $\beta-\beta'$ )	7.75–7.30, m, 6H ( <i>meta, para</i> )	7.60–7.45, br, 9H ( <i>meta, para</i> )	6.96–6.94, m, 3H ( <i>meta, para</i> )	25.34, d, $J = 454$ Hz

<sup>a</sup> Spectra recorded at 300 MHz in DMF-*d*<sub>7</sub> at room temperature. Chemical shifts are reported in ppm downfield of tetramethylsilane but assigning the residual  $^1\text{H}$  signal of the deuterated solvent at 7.24 ppm. <sup>b</sup> Spectra recorded at 121 MHz in DMF-*d*<sub>7</sub> at room temperature. Chemical shifts are reported downfield of external 85% H<sub>3</sub>PO<sub>4</sub>.

**Scheme 2**

appeared at 6.96–6.94 and 6.51–6.47 ppm, due to the *meta* and *ortho-para* protons of the newly entered Ph group.

Variations in the  $\{^1\text{H}\}^{31}\text{P}$  NMR spectrum also accounted for the transmetalation process. The two nonequivalent phosphorus atoms of **3** give rise to two doublets at 35.55 and 17.00 ppm. The large coupling constant ( $J_{\text{P-P}} = 456$  Hz) is typical of unequivalent phosphorus atoms arranged in a *trans* fashion on a metal center.<sup>10</sup> Upon formation of **5**, these two doublets were shifted to 35.80 and 25.34 ppm. The large value of the coupling constant ( $J_{\text{P-P}} = 454$  Hz) indicates that the *trans* geometry is retained in the new species. The formation of Me<sub>3</sub>SnI, detected by GC/MS, confirmed the occurrence of the transmetalation process.

Because of the clear spectroscopic evidence for the formation of **5**, we were urged to design a more suitable model that would also allow the isolation of the transmetalation product.

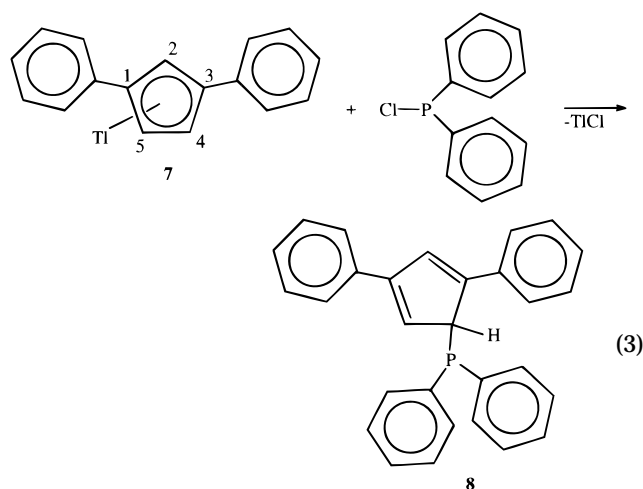
We turned our attention to the use of a substituted  $\eta^5$ -Cp ligand that, while maintaining the key presence of the chelating diphenylphosphino arm, bore bulky substituents that would make the products more robust and easier to handle. This idea was pursued by using the 1-(diphenylphosphino)-2,4-diphenylcyclopentadienide ligand **9**, relying on the expectation that, without altering the reactivity pattern under investigation, the

introduction of two phenyl groups into the Cp ring could impart a certain degree of kinetic stabilization to these otherwise thermodynamically unstable intermediates.

**Formation of ( $\eta^5$ -1-Ph<sub>2</sub>P-2,4-Ph<sub>2</sub>C<sub>5</sub>H<sub>2</sub>)(CO)<sub>3</sub>MI (M = Mo, **12**; W, **13**).** Complexes **12** and **13** were obtained by the procedure we previously used to form the corresponding analogs **1** and **2**. A much better overall yield, improved product stability, and simpler synthetic procedure rewarded the use of the 1-(diphenylphosphino)-2,4-diphenylcyclopentadienide ligand with respect to results from the use of the (diphenylphosphino)cyclopentadienide. The synthetic route started by reacting an ethereal suspension of 1,4-diphenyl-1,3-cyclopentadiene (**6**) with 1 equiv of TlOEt at room temperature (Scheme 2). Upon mixing reactants, a bright yellow precipitate of ( $\eta^5$ -1,3-diphenylcyclopentadienyl)thallium (**7**) was immediately formed. Once prepared, the thallium derivative **7** could be either directly used to form **12** or **13** or isolated and stored in the refrigerator inside a glovebox for later use, with unchanged efficiency. In the straightforward preparation, following filtration, the solid residue was dissolved in THF and treated with ClPPh<sub>2</sub>. A tan precipitate of TlCl was formed and separated from the solution containing the diphenylphosphino derivative **8**. Direct addition at room temperature of a stoichiometric amount of BuLi to the THF solution of **8** led to the formation of the

lithium salt **9**, which was then treated with solid  $(\text{CH}_3\text{CN})_3\text{M}(\text{CO})_3$  ( $\text{M} = \text{Mo}, \text{W}$ ). In the case of the formation of **10**, the initial slurry turned to a deep yellow-brown solution, while the formation of **11** was accompanied by the formation of a red-purple solution. After overnight stirring at room temperature, followed by a 1 h reflux, the complete formation of **10** and **11** was checked by IR.<sup>9b,11</sup> After cooling, the addition of 1,2-diiodoethane to **10** and **11** led to the formation of **12** and **13**, respectively. Chromatographic separation on silica gel column afforded the pure products in 98% and 79% overall yields, respectively.

Although, in principle, two different products are possible from reaction of **7** with  $\text{ClPPh}_2$ , one arising from the attack of the phosphorus in position 2 of the Cp ring, and the other from the attack of one of the two equivalent positions 4 or 5 (eq 3), the  $^1\text{H}$  NMR spectrum of the final products accounted for the exclusive formation of **12** and **13**. This shows that the steric hindrance

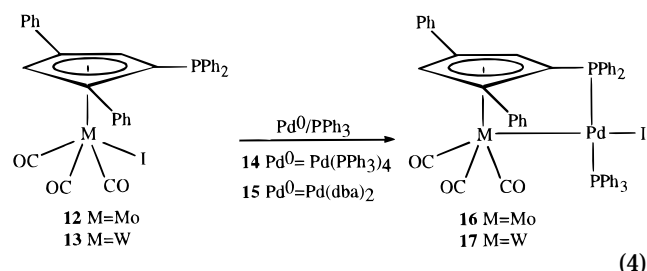


of the two phenyl groups disfavors the addition at carbon C2; consequently, attack can be directed only on the 4 or 5 position, generating in both cases product **8**.

Both **12** and **13** have been characterized by spectroscopy and microanalysis. Complex **13** has been also structurally characterized by single-crystal X-ray diffraction (Figure 3).

#### Reaction of **12** and **13** with Zerovalent Palladium. Formation of the Oxidative Addition

**Products**  $(\eta^5\text{-1-Ph}_2\text{P-2,4-Ph}_2\text{C}_5\text{H}_2)(\text{CO})_3\text{MPd}(\text{PPh}_3)\text{I}$  ( $\text{M} = \text{Mo}$ , **16**;  $\text{M} = \text{W}$ , **17**). Complexes **12** and **13** smoothly undergo oxidative addition on zerovalent palladium, forming the corresponding products **16** and **17** (eq 4). Reaction occurs at room temperature in THF



(11) **10**: IR (THF,  $\nu_{\text{CO}}$ ) 1906 (vs), 1816 (vs), 1789 (s), 1733 (s)  $\text{cm}^{-1}$ .  
**11**: IR (THF,  $\nu_{\text{CO}}$ ) 1924 (vs), 1902 (vs), 1812 (s), 1732 (s)  $\text{cm}^{-1}$ .

**Table 2.** Crystallographic Information

complex	<b>13</b>	<b>17</b>
formula	$\text{C}_{36}\text{H}_{30}\text{IO}_4\text{PW}$	$\text{C}_{54}\text{H}_{45}\text{IO}_4\text{P}_2\text{PdW}$
crystal		
color	colorless	colorless
shape	prism	prism
dimensions(mm)	$0.31 \times 0.43 \times 0.76$	$0.09 \times 0.17 \times 0.28$
crystal system	orthorhombic	monoclinic
space group	<i>Pbca</i>	<i>P2<sub>1</sub>/n</i>
cell constants		
<i>a</i> (Å)	29.035(2)	24.078(3)
<i>b</i> (Å)	12.545(3)	16.085(2)
<i>c</i> (Å)	18.640(2)	12.289(3)
α (deg)	90	90
β (deg)	90	93.31(4)
γ (deg)	90	90
cell determination		
no. of reflections	42	43
θ range (deg)	5.6–17.4	5.1–13.2
cell volume (Å <sup>3</sup> )	6789.51	4730.63
formula units	8	4
<i>D</i> <sub>calc</sub> (g cm <sup>-3</sup> )	1.70	1.74
μ <sub>calc</sub> (cm <sup>-1</sup> )	44.57	36.14
diffractometer	Philips PW1100	Philips PW1100
radiation, wavelength (Å)	Mo Kα, 0.710 69	Mo Kα, 0.710 69
standard reflection, step	one, every 100	one, every 100
decay of standard	13%	19%
independent reflections	7362	10 312
measured		
reflections observed	2725 ( <i>x</i> = 4)	2154 ( <i>x</i> = 4)
[ <i>I</i> > <i>xσ</i> ( <i>I</i> )]		
θ range (deg)	3–30	3–27
indices range: <i>h, k, l</i>	0/37, 0/16, 0/23	–30/30, 0/20, 0/15
no. of refined parameters	487	284
<i>R</i>	0.044	0.043
weights	unitary	unitary
Δ <i>Q</i> <sub>min/max</sub> (e/Å <sup>-3</sup> )	–0.96/1.85	–3.44/1.16
min/max absorb	0.90/1.31	0.75/1.99
corr factors		

by stirring overnight **12** or **13** in the presence of an equivalent amount of  $\text{Pd}(\text{PPh}_3)_4$  (**14**) or  $\text{Pd}(\text{dba})_2$  (**15**). In the latter case, an equivalent amount of  $\text{PPh}_3$  was added to the reaction mixture in order to provide the ancillary ligand needed to stabilize the palladium center in products **16** and **17**. Isolation of pure products, performed by chromatographic separation, was much easier when the combination  $\text{Pd}(\text{dba})_2/\text{PPh}_3$  was used, because of the absence of the troublesome excess of  $\text{PPh}_3$  present in the reaction mixture when  $\text{Pd}(\text{PPh}_3)_4$  was used. Chromatographic separation on silica gel afforded air-stable pure **16** and **17** in 92% and 68% yields, respectively.

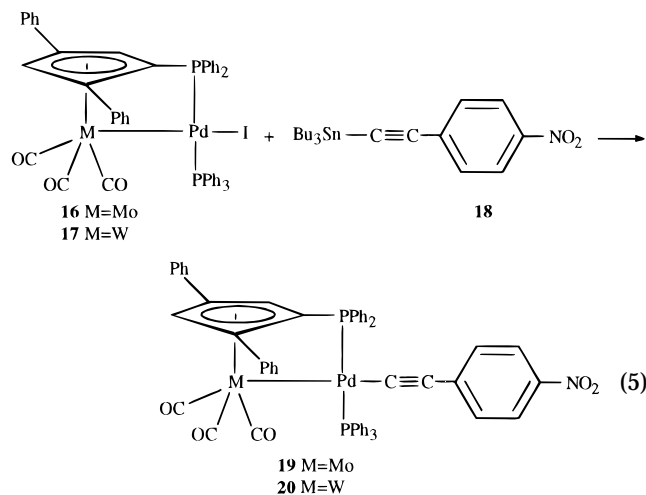
To better understand the structural features of these  $\text{M-Pd-I}$  complexes, we have investigated the molecular structure of **17** by single-crystal X-ray analysis. The results of the single-crystal X-ray diffraction study are summarized in Table 2, and a plot of **17** with thermal ellipsoids is displayed in Figure 4.

#### Reaction of **16** and **17** with Stannylacetylides. Formation of the Transmetalation Products $(\eta^5\text{-1-Ph}_2\text{P-2,4-Ph}_2\text{C}_5\text{H}_2)(\text{CO})_3\text{MPd}(\text{PPh}_3)\text{C}\equiv\text{C}(\text{C}_6\text{H}_4)\text{p-NO}_2$ ( $\text{M} = \text{Mo}$ , **19**; $\text{M} = \text{W}$ , **20**).

Once the oxidative addition process was clearly assessed with the isolation of **16** and **17**, we took advantage of the easy access to such important intermediates to further explore the dynamic of the Pd-catalyzed metal–carbon bond formation. Referring to Figure 1, the second step occurring in the Pd-catalyzed carbon–carbon bond formation is the transmetalation occurring between the oxidatively

added intermediate and a nucleophile such as an organostannane.

Both the Mo–Pd and the W–Pd complexes **16** and **17** were then reacted with some representative ethynyltin derivatives. Although we found that several (phenylethynyl)trialkyltin derivatives which carried different substituents on the phenyl ring successfully underwent the transmetalation reaction,<sup>12</sup> we report here only the case of the 4-nitro-1-[2-(tributyltin)ethynyl]benzene (**18**), which was the most suitable to afford stable transmetalation products (eq 5). An



important effect of the solvent was noticed in this transformation. In THF, reactions are slow and incomplete. Even with the use of a 5-fold excess of the acetylenic stannane and prolonged reaction time, consistent amounts of starting material remained unchanged, both in the cases of the Mo–Pd and the W–Pd complexes. Conversely, reaction of **16** and **17** with a slight excess of the tin acetylide **18** in DMF goes to completion within minutes, and following workup, products **19** and **20** were isolated in 86% and 90% yields, respectively. Unfortunately, despite several attempts, no X-ray quality material was obtained.

**NMR.** Despite some limitations, the NMR technique was revealed to be a particularly suitable tool for the study of the phenomenon described in this work (Table 3). In the complexes we studied, limitations resulted from the presence of a large number of nonequivalent phenyl groups, in which <sup>1</sup>H and <sup>13</sup>C NMR resonances were further complicated by coupling with two nonequivalent phosphorus groups, resulting in the display of complicated sets of overlapping signals. Moreover, the limited solubility of these complexes prevented the recording of understandable <sup>13</sup>C NMR spectra. In spite of these facts, <sup>1</sup>H NMR signals of the sole two cyclopentadienyl protons and <sup>31</sup>P NMR spectra allowed a clear understanding of the transformations under investigation.

In the following, we shall discuss only some key NMR features relative to the molybdenum complexes **12**, **16**, and **19**, those of the corresponding tungsten complexes being similar.

The <sup>1</sup>H NMR spectrum of **12** shows, for the two Cp protons, two sets of well-separated signals, a quartet at 6.41 and a doublet at 5.49 ppm. The downfield signal

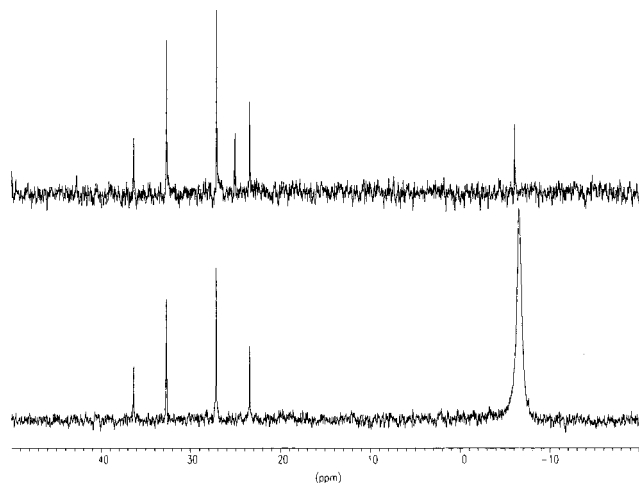


**Figure 2.** <sup>31</sup>P{<sup>1</sup>H} NMR spectra at 121 MHz of complex **20**. Upper trace, spectra recorded after dissolution of the compound in CDCl<sub>3</sub> at room temperature. Lower trace, spectra recorded after addition of an excess of PPh<sub>3</sub>.

is relative to the α proton adjacent to the phosphorus atom and is more affected by its deshielding effect,<sup>13</sup> while the upfield signal belongs to the β proton. The <sup>31</sup>P NMR spectrum of **12** shows a sharp singlet at –21.31 ppm.

Formation of **16** was evidenced by an upfield shift of the two Cp protons, the resonances of which now appear as triplets at 6.07 ppm for the H<sub>α</sub> and at 4.54 ppm for the H<sub>β</sub>. The <sup>31</sup>P NMR spectrum of **16** much more dramatically accounts for the structural variations taking place with the introduction of the Pd and its ancillary PPh<sub>3</sub> on **12** (eq 4). In **16**, the two nonequivalent phosphorus atoms bonded to palladium in *trans* configuration give rise to a simple first-order AB splitting pattern, which produces two sets of doublets, centered at 39.23 and 17.49 ppm, respectively, with a coupling constant of 458 Hz.

On formation of **19**, the two Cp protons were only slightly influenced, while significant variations were observed for the phenyl protons. In **18**, they appear as two doublets at 8.09 and 7.50 ppm (*J* = 9.03 Hz), while in **19** they were shifted to 7.69 and 6.27 ppm (*J* = 8.7 Hz). The <sup>31</sup>P NMR spectrum of **19** shows that, with respect to **16**, the two doublets slightly changed their chemical shift to 39.67 and 26.25 ppm while maintaining a coupling constant of 448 Hz. This accounts for formation of a new species, still possessing the two phosphorus group in the *trans* feature as in **16**. By comparing the <sup>31</sup>P NMR data reported in Tables 1 and 3, it is evident that NMR variations occurring with formation of **16** and **19** (eqs 4 and 5) are similar to those observed upon formation of **3** and **5** (eqs 1 and 2).

An interesting feature was observed on recording the <sup>31</sup>P NMR spectrum of the tungsten complex **20** (Figure 2). Upon dissolving a sample of product in CDCl<sub>3</sub>, the <sup>31</sup>P NMR spectrum showed, along with the expected pattern for the product (Table 3), two singlets at 25.08 and –6.17 ppm. Observing that the signal at lower field was characteristic of the free triphenylphosphine ligand, we attributed the singlet at 25.08 ppm to the trigonal complex **21** that may be formed by dissociation of PPh<sub>3</sub>

(13) (a) Mathey, F.; Lampin, J. P. *Tetrahedron* **1975**, *31*, 2685. (b) Casey, C. P.; Bullock, R. M.; Fultz, W. C.; Rheingold, A. L. *Organometallics* **1982**, *1*, 1591.

(12) Narducci, V.; Cianfriglia, P.; Lo Sterzo, C. Work in progress.

Table 3.  $^1\text{H}$  and  $^{31}\text{P}$  NMR and IR Data for Complexes 12, 13, 16, 17, 19, and 20

	$^1\text{H}$ NMR <sup>a</sup>	$^{31}\text{P}$ NMR <sup>b</sup>	IR <sup>c</sup>	$^1\text{H}$ NMR <sup>a</sup>	$^{31}\text{P}$ NMR <sup>b</sup>	IR <sup>c</sup>	
	<b>12, M = Mo</b>			<b>13, M = W</b>			
	6.41, dd, 1H, $J_{\text{HH}} = 2.3$ Hz ( $\alpha$ ) $J_{\text{PH}} = 1.5$ Hz ( $\alpha$ ) 5.49, d, 1H, $J_{\text{HH}} = 2.3$ Hz ( $\beta$ )	-23.31, s	2039.5 (s) 1967.1 (s)	6.45, dd, 1H, $J_{\text{HH}} = 2.2$ Hz ( $\alpha$ ) $J_{\text{PH}} = 1.2$ Hz ( $\alpha$ ) 5.53, d, 1H, $J_{\text{HH}} = 2.2$ Hz ( $\beta$ )	-19.68, s	2033.9 (s) 1952.9 (s)	
	<b>16, M = Mo</b>			<b>17, M = W</b>			
	6.07, t, 1H, $J = 2.1$ Hz ( $\alpha$ ) 4.54, t, 1H, $J = 2.5$ Hz ( $\beta$ )	39.23, d, $J = 458$ Hz 17.49, d, $J = 458$ Hz	1965.0 (s) 1866.2 (s) 1137.5 (s) 1096.4 (m)	6.01, t, 1H, $J = 1.9$ Hz ( $\alpha$ ) 4.61, t, 1H, $J = 2.2$ Hz ( $\beta$ )	30.19, d, $J = 460$ Hz 15.82, d, $J = 460$ Hz	1960.7 (s) 1884.2 (s) 1861.2 (s)	
	<b>19, M = Mo</b>			<b>20, M = W</b>			
	6.13, t, 1H, $J = 2.1$ Hz ( $\alpha$ ) 4.73, t, 1H, $J = 2.4$ Hz ( $\beta$ )	39.67, d, $J = 458$ Hz 26.25, d, $J = 458$ Hz	1950.8 (s) 1872.7 (m) 1845.6 (s) 1512.8 (m) 1338.3 (m)	6.06, t, 1H, $J = 2.0$ Hz ( $\alpha$ ) 4.74, t, 1H, $J = 2.1$ Hz ( $\beta$ )	34.28, d, $J = 450$ Hz 25.27, d, $J = 450$ Hz	2102.5 (w) 1946.5 (s) 1864.3 (m) 1840.1 (s) 1512.9 (s) 1338.0 (s)	

<sup>a</sup> Spectra recorded at 300 MHz in  $\text{CDCl}_3$  at room temperature. Chemical shifts are reported in ppm downfield of tetramethylsilane but assigning the residual  $^1\text{H}$  signal of the deuterated solvent at 7.24 ppm. <sup>b</sup> Spectra recorded at 121 MHz in  $\text{CDCl}_3$  at room temperature. Chemical shifts are reported downfield of external 85%  $\text{H}_3\text{PO}_4$ . <sup>c</sup> Spectra obtained in  $\text{CH}_2\text{Cl}_2$  at room temperature.

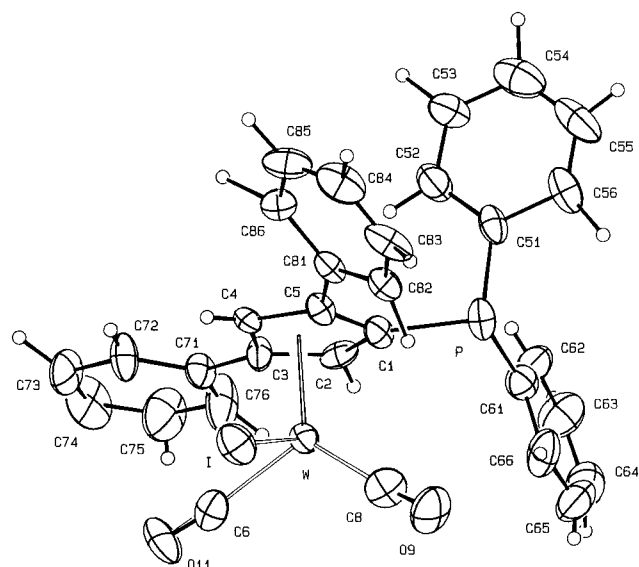
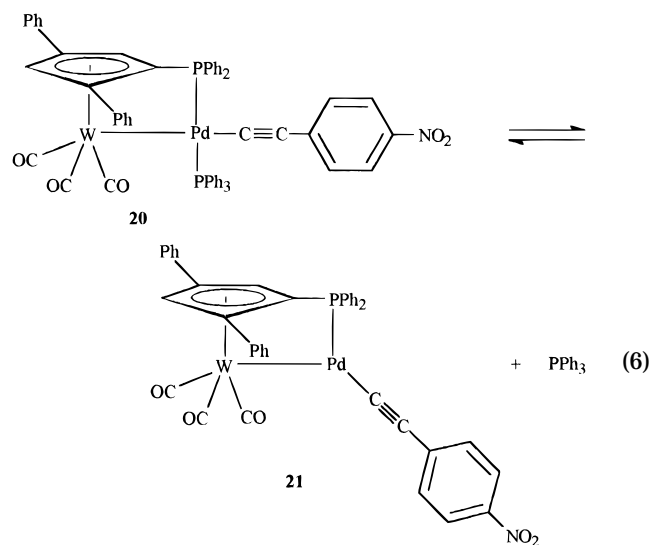


**Figure 3.** Geometry of the complex  $[\eta^5\text{-1-Ph}_2\text{P-2,4-Ph}_2\text{C}_5\text{H}_2](\text{CO})_3\text{WI}$  (**13**) showing the atomic labeling scheme. The solvent and disordered atoms were omitted for clarity. The ORTEP diagram is with 30% probability contours of vibration ellipsoids.

from **20** (eq 6). Addition of an excess of  $\text{PPh}_3$  to the NMR tube completely suppressed the signal at 25.08 ppm, thus indicating that the new species has completely reversed to **20**.



**X-ray Structures.** Drawings of the molecular structures of complexes **13** and **17** with their respective labeling schemes are in given Figures 3 and 4. Table 4 reports selected geometrical parameters for the two complexes. In **13**, the tricarbonyl iodine moiety, coordinated by the W atom, shows a disorder consisting of mutually interchanged positions of the iodine with the  $\text{C7}=\text{O10}$  group, having occupancy values of 0.52 and 0.48, respectively.

The  $\text{W}-\text{C}_{\text{Cp}}$  distances are irregular, ranging from 2.295(8) to 2.381(8) Å in **13** and from 2.324(10) to 2.352(11) Å in **17**. The increased lengths of some bond distances of the Cp rings may reflect the steric crowding between the aromatic substituents and the diphenylphosphine moiety, which assumes a different orientation in **17** for coordination with palladium. When **13**

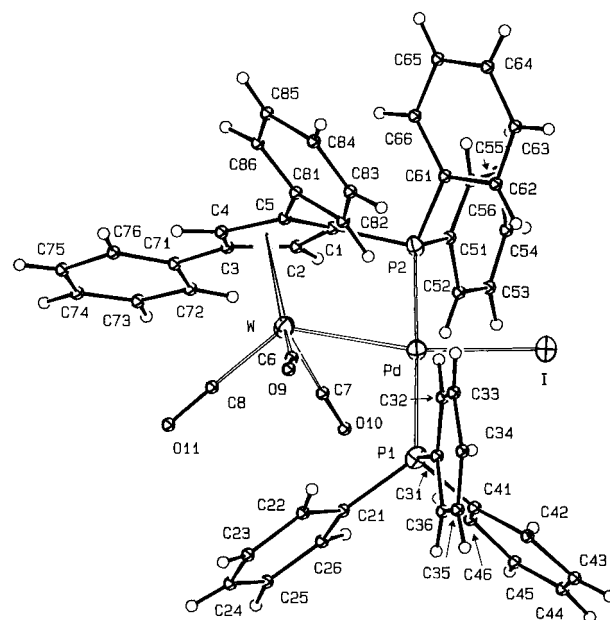


**Figure 4.** Geometry of the complex  $[\eta^5\text{-1-Ph}_2\text{P-2,4-Ph}_2\text{C}_5\text{H}_2](\text{CO})_3\text{WPd}(\text{PPh}_3)\text{I}$  (**17**) showing the atomic labeling scheme. The solvent atoms were omitted to have more evidence. The ORTEP diagram is with 30% probability contours of vibration ellipsoids.

**Table 4.** Selected Bond Distances (Å) and Angles (deg)

bond	<b>13</b>	<b>17</b>	angle	<b>13</b>	<b>17</b>
W-Pd		2.831(1)	Cp-W-I	115.5(1)	
W-Cp	2.009(1)	2.003(1)	Cp-W-I'	113.8(1)	
W-C6	2.072(10)	1.917(12)	Cp-W-C6	122.5(3)	124.7(4)
W-C7	2.030(25)	1.938(13)	Cp-W-C7	109.1(6)	124.9(4)
W-C7'	2.044(33)		Cp-W-C8	126.5(3)	120.9(4)
W-C8	2.026(11)	1.945(12)	C6-W-C7	80.2(7)	107.5(5)
W-I	2.784(2)		C6-W-C8	111.0(4)	83.5(5)
W-I'	2.774(2)		C7-W-C8	78.8(6)	80.4(5)
Pd-I		2.665(2)	C7-W-I'	137.1(7)	
Pd-P1		2.384(3)	C7'-W-I	137.2(9)	
Pd-P2		2.280(3)	Pd-W-Cp		109.0(1)
P-C1	1.820(8)	1.782(11)	Pd-W-C6		71.4(4)
P-C21		1.874(12)	Pd-W-C7		67.0(4)
P-C31		1.822(11)	Pd-W-C8		129.9(4)
P-C41		1.785(13)	W-Pd-I		166.7(1)
P-C51	1.820(9)	1.781(11)	W-Pd-P1		102.7(1)
P-C61	1.822(10)	1.856(12)	W-Pd-P2		76.5(1)
C6-O9	1.013(13)	1.194(14)	I-Pd-P1		89.8(1)
C7-O10	1.091(44)	1.202(16)	I-Pd-P2		91.1(1)
C7'-O10'	1.040(43)		P1-Pd-P2		178.4(1)
C8-O11	1.092(13)	1.198(16)	Pd-P1-C21		123.6(4)
C1-C2	1.387(12)	1.402(15)	Pd-P1-C31		108.8(4)
C1-C5	1.413(11)	1.502(15)	Pd-P1-C41		112.3(4)
C2-C3	1.393(12)	1.463(15)	Pd-P2-C1		105.0(4)
C3-C4	1.436(12)	1.380(15)	Pd-P2-C51		113.2(4)
C3-C71	1.461(11)	1.489(16)	Pd-P2-C61		124.0(4)
C4-C5	1.433(11)	1.457(16)	C1-P2-C51	99.9(4)	103.0(5)
C5-C81	1.484(12)	1.497(16)	C1-P2-C61	128.8(6)	124.8(8)
			P2-C1-C5	126.0(6)	122.6(8)

and **17** are compared, the most striking evidence is the heavy distortion of the general molecular framework around the tungsten center upon insertion of palladium and the formation of the four-membered bimetallic ring

$\text{Cp}-\text{W}-\text{Pd}-\text{P}$  (assuming the whole Cp participated as a single unit of this ring). A strong bonding interaction exists between W and Pd, which are linked at a distance of 2.831(1) Å, significantly shorter than the sum of the corresponding covalent radii (2.986 Å).<sup>14a</sup> The presence of this Pd-W bond represents the key feature deter-

mining the overall arrangement of the entire molecule. In **13** the P atom is out 0.149(2) Å from the plane of the  $\eta^5$ -Cp ligand. In **17**, the coordination with the Pd lowers this P 0.575(3) Å below the Cp plane. Because of the short distance between the two metals, the ancillary triphenylphosphine linked to the palladium exerts a relevant steric pressure on the W(CO)<sub>3</sub> tripod, imposing a deviation up to 10.7° of the W–C=O groups from linearity. For the same reason, the P atom linked to the Cp decreases its distance from C1 from 1.820(8) Å in **13** to 1.782(11) Å in **17**, with a consequent increase of the steric influence of the diphenylphosphino group on the nearby phenyl ring linked to the C2. To relieve this hindrance, the C1–C5 distance is stretched from 1.413(11) Å in **13** to 1.502(15) Å in **17**. In **13**, the plane of the phenyl group linked to the C2 because of the presence of the adjacent diphenylphosphino moiety shows a dihedral angle of 40.8(3)° with respect to the Cp plane, while the phenyl ring linked to the C4, free of any steric influence, is rotated by an angle of only 4.9(4)° with respect to the Cp plane. In **17**, the tilt of the phenyl group in C2 rises to 50.0(4)°, while the phenyl group in C4 increases to 10.4(4)° its deviation from the Cp plane. For the phenyl in C2, we relate these variations with the closer distance of this group to the diphenylphosphino moiety, while the phenyl in C4 increases its deviation from the Cp plane because of the steric pressure exerted by the distorted W(CO)<sub>3</sub> tripod.

Relevant variations from ideal geometry are also observed around the Pd center. The W–Pd–P1 and the W–Pd–P2 angles deviate to 102.7(1)° and 76.1(1)°, far from the 90° expected for a normal square planar coordination around Pd. Moreover, the Cp–W–Pd angle found at 109.0(1)° strongly differs from the values of the other bond angles observed between the Cp–W axis and the three W–CO bonds (120–124°). This strong deformation from regular values occurring at bond angles and distances of **17** upon formation of the W–Pd bond accounts for the strong interaction existing between these two metals. It is important to note that a computer-assisted literature search revealed that the Pd–W bond as it is shown in **17** is a very rare feature, with only few precedents.<sup>14</sup> The Pd–I bond length is longer than that found for other comparable distances.<sup>15,16</sup> This elongation may be ascribed to the steric hindrance with PPh<sub>3</sub> and PPh<sub>2</sub> groups and to the *trans* effect of the Pd–W and Pd–I. Similar lengthening of terminal halide–metal bonds, *trans* to metal–metal bonds, has been seen before.<sup>17</sup>

In the solid state, both molecules are connected by van der Waals forces.

### Discussion

During our first approach to the study of the mechanism of the Pd-catalyzed metal–carbon bond forma-

tion, we found that the use of the (diphenylphosphino)cyclopentadienyl bidentate ligand enabled the isolation of the M–Pd–I complexes **3** and **4**, formed upon reaction of M–I moieties (M = Mo, W) with zerovalent palladium<sup>10</sup> (eq 1). This result, described as an oxidative addition process, showed an intriguing analogy with the first step, often crucial, of the mechanism of the Pd-catalyzed carbon–carbon bond formation.<sup>7</sup> Unfortunately, preparation of starting materials required cumbersome procedures, and isolation of the product was difficult and unreliable, because of the instability of the M–Pd–I complexes **3** and **4**.<sup>10</sup> Moreover, we could only obtain spectroscopic evidences of the consequence of their reaction with (phenylethynyl)trimethyltin. These results urged the search for a more suitable model to get insight into the mechanism of the phenomenon we were investigating.

The replacement of the (diphenylphosphino)cyclopentadiene ligand with the 1-(diphenylphosphino)-2,4-diphenylcyclopentadienide satisfied this expectation by improving product stability without depressing reactivity.<sup>18a</sup> Thus, the starting metal iodides **12** and **13** were straightforwardly obtained by an identical and simplified synthetic route (Scheme 2), while **1** and **2** required the design of two different synthetic approaches.<sup>10</sup> Moreover, in sharp contrast with the difficulties encountered with the isolation of **3** and **4**, **12** and **13** smoothly formed the products of oxidative addition **16** and **17**, which were easily purified by chromatographic separation. The improved stability of both the otherwise labile M–I and M–Pd–I species, accompanied by the unchanged reactivity, suggested that the two phenyl groups attached to the Cp ring in **12** and **13** may operate some electronic effect influencing the electrophilic character of the M–I moiety. In this respect, although it remains a delicate matter to assess to what extent the two phenyl groups on the Cp operate a charge delocalization from the metal through the Cp ring,<sup>18b,c</sup> it is important to observe from the X-ray data of **13** the arrangement of the two phenyl groups bonded on the Cp (Figure 3). The phenyl in position 2, because of the presence of the adjacent bulky diphenylphosphino group, suffers a 40.3(3)° deviation from coplanarity with the Cp plane, while the phenyl group in position 4, free from any steric compression, almost aligns its plane to the Cp ring plane [4.9(4)° of deviation] in the position for operating electronic conjugation with the Cp ring, thus influencing charge and electron density on the metal.

It is important to note that, while the formation of the M–Pd–I complexes **3**, **4**, **16**, and **17** clearly accounts for an oxidative addition of M–I moieties on zerovalent palladium, one can envision this as a peculiar characteristic of the substrate we used without any relevance to the mechanism of the Pd-catalyzed metal–carbon bond formation. In this respect, a number of literature reports account for the formation of M–Pd–X arrays in which palladium is inserted in a variety of fashions between a transition metal (M) and a halide (X), and in some cases their formation has been rationalized as an oxidative addition of M–X moieties to zerovalent palladium.<sup>3a,10</sup> Moreover, with the formation of the

(14) (a) Bender, R.; Braunstein, P.; Jud, J.-M.; Dusausoy, Y. *Inorg. Chem.* **1983**, *22*, 3394 and references therein. (b) Howard, K. E.; Rauchfuss, T. B.; Wilson, S. R. *Inorg. Chem.* **1983**, *27*, 3561. (c) Zhengzhi, Z.; Xukun, W.; Yujun, S.; Xinkan, Y.; Honggen, W. *Gaodeng Xuexiao Huaxue Xuebao (Chem. J. Chin. Univ.)* **1990**, *11*, 255. (d) Engel, P. F.; Pfeffer, M.; Fischer, J.; Dedieu, A. *J. Chem. Soc., Chem. Commun.* **1991**, 1274. (e) Engel, P. F.; Pfeffer, M.; Fischer, J. *Organometallics* **1994**, *13*, 4751.

(15) Hirschon, A. S.; Musker, W. K.; Olmstead, M. M.; Dallas, J. L. *Inorg. Chem.* **1981**, *20*, 1702.

(16) Bailey, N. A.; Mason, R. *J. Chem. Soc. A* **1968**, 2594.

(17) Farr, J. P.; Olmstead, M. M.; Balch, A. L. *Inorg. Chem.* **1983**, *22*, 1229.

(18) (a) Janiak, C.; Schumann, H. *Adv. Organomet. Chem.* **1991**, *33*, 291. (b) Evans, D. A.; Chapman, K. T.; Bisaha, J. *J. Am. Chem. Soc.* **1984**, *106*, 4261. (c) Broadley, K.; Lane, G. A.; Connelly, N. G.; Geiger, W. E. *J. Am. Chem. Soc.* **1983**, *105*, 2486.



M–Pd–I complexes, the metal–iodo moiety has certainly been activated, but other critical key steps need to be realized in order to complete the catalytic cycle.<sup>19</sup> However, convincing evidence that the process we are studying plays a role in the formation of a metal–carbon bond promoted by palladium arises from the smooth reaction occurring between the oxidative addition intermediates **16** and **17** and the acetylenic stannane **18**, to form the products of transmetalation, **19** and **20** (eq 5). In reference to the mechanism of the Pd-catalyzed carbon–carbon bond formation, although the oxidative addition step is the trigger of the whole catalytic cycle,<sup>7</sup> transmetalation is almost invariably the rate-limiting step, and generally, when the oxidative addition–transmetalation–reductive elimination sequence fails, it is this step which warrants attention.<sup>1,7,20</sup> In **19** and **20**, the metal center M and the acetylide, i.e., the two partners to be coupled, although joined by the interposition of palladium, constitute already a single molecular unit, and the completion of the coupling process through the *trans* to *cis* isomerization and the reductive elimination steps is expected to be an overall downhill energetic pathway. In this respect, the behavior of **20** is noteworthy. During the recording of its <sup>31</sup>P NMR spectrum, it showed a behavior similar to the reversible formation of the trigonal complex **21** (eq 6), which may be the precursor to the *cis* isomer. In the carbon–carbon coupling reaction, the formation of a similar trigonal complex has been already invoked as intermediate during the *trans* to *cis* isomerization preceding reductive elimination.<sup>7b,21</sup>

Preliminary evidence that these complexes further evolve toward the completion of the catalytic cycle has already been obtained.<sup>12</sup>

### Conclusion

In conclusion, with the isolation of the oxidative addition and transmetalation intermediates **16**, **17**, and **19**, **20**, we showed impressive analogies between the Pd-catalyzed *carbon–carbon* and *metal–carbon* bond formation mechanisms, and these results suggest that this second pathway could disclose the feasibility of a similar efficient and useful chemistry as that of the former process. Moreover, the model we engineered in the present study, by allowing a large degree of systematic variations, seems particularly suitable to carry out systematic and quantitative investigations of the processes under examination. One can study the dependence of the various steps of these transformations from steric and electronic factors, by varying the type of ancillary ligands, both on the metal M and the Pd, and the number and type of the substituents on the Cp as well as on the coordinating side arm. The easy isolation of the oxidative addition intermediate should also allow its use for systematic screening of the transmetalation process, taking advantage of the easy availability of a large variety of organotin partners.<sup>6</sup> These studies, besides clarifying the factors influencing the metal–carbon formation phenomenon, by reversing the parallelism, might also shed light on many still unclear

aspects of the carbon–carbon coupling itself, for which important reinterpretations have been proposed.<sup>5,7</sup> Moreover, it is also worthy of note that, while the Mo–Pd bond is quite a common feature, complexes such as **4**, **17**, and **20** add to the very few existing examples showing a direct W–Pd bond.<sup>14</sup> In our opinion, the successful isolation of complexes **19** and **20** represents, indeed, the disclosure of a new scenario in the endless world of surprises of palladium chemistry.

### Experimental Section

**Reagents and Methods.** Elemental analyses were performed by the Servizio Microanalisi of the Area della Ricerca di Roma (C.N.R., Montelibretti, Italy).

Solvents, including those used for chromatography, and liquids were thoroughly degassed before use. Flash chromatography was performed with 230–400 mesh silica gel (Merck).

All reactions were carried out under an atmosphere of prepurified argon using conventional vacuum line and Schlenk tube techniques<sup>22</sup> in oven-dried glassware, or in a nitrogen-filled Braun glovebox. Liquids were transferred by syringe or cannula techniques. THF and Et<sub>2</sub>O were distilled from sodium–potassium alloy. DMF was distilled from CaH<sub>2</sub> under reduced pressure. Preparation of the 1,3-diphenyl-2,4-cyclopentadiene required modification of the literature report.<sup>23</sup> The crude ethyl 3-benzoylpropionate precursor had to be formed using an excess of ethyl alcohol and then dissolved in Et<sub>2</sub>O and washed to neutrality with an ice-cold solution of NaHCO<sub>3</sub> to remove the remaining alcohol and the H<sub>2</sub>SO<sub>4</sub> used to catalyze its formation. Without these precautions, formation of the ester was incomplete, and extensive decomposition took place during distillation. Moreover, the subsequent cyclization step must be performed by using the minimum amount of benzene solvent so as to obtain a 1 M solution of EtONa. Bis(dibenzylideneacetone)palladium [Pd(dba)<sub>2</sub>],<sup>24</sup> (CH<sub>3</sub>CN)<sub>3</sub>Mo(CO)<sub>3</sub>,<sup>25</sup> (CH<sub>3</sub>CN)<sub>3</sub>W(CO)<sub>3</sub>,<sup>25</sup> Pd[P(C<sub>6</sub>H<sub>5</sub>)<sub>3</sub>]<sub>4</sub>,<sup>26</sup> (CH<sub>3</sub>)<sub>3</sub>SnC≡CC–H<sub>5</sub>,<sup>27</sup> HC≡C(C<sub>6</sub>H<sub>4</sub>)*p*-NO<sub>2</sub>,<sup>28</sup> and Bu<sub>3</sub>SnNEt<sub>2</sub><sup>29</sup> were prepared according to published procedures.

TIOCH<sub>2</sub>CH<sub>3</sub> (Aldrich), CIP(C<sub>6</sub>H<sub>5</sub>)<sub>2</sub> (Strem), and ICH<sub>2</sub>CH<sub>2</sub>I (Aldrich) were used as received. The active organometallic content of the organolithium reagents was checked periodically by titration with 2,5-dimethoxybenzyl alcohol.<sup>30</sup>

( $\eta^5$ -2,4-Ph<sub>2</sub>C<sub>5</sub>H<sub>3</sub>)Ti (**7**). This compound was prepared by adopting the method developed by Mathey and Lampin<sup>13</sup> for a similar compound. A 500 mL Schlenk flask was loaded with 17.85 g (81.78 mmol) of **6** and 400 mL of ethyl ether. To this was added 20.4 g (81.78 mmol) of thallium ethoxide by a syringe, causing the formation of a yellow precipitate. After 1 h of stirring, the suspension was filtered and the solid washed with ethyl ether (3 × 20 mL) and then dried under vacuum to afford 33.44 g (97%) of product.

<sup>1</sup>H NMR (DMSO-*d*<sub>6</sub>):  $\delta$  5.39 (d, 2H, *J* = 2.2 Hz), 5.89 (t, 1H, *J* = 2.2 Hz), 6.17 (t, 2H, *J* = 7.7 Hz), 6.41 (t, 4H, *J* = 7.7 Hz), 6.59 (d, 4H, *J* = 7.7 Hz). <sup>13</sup>C NMR (DMSO-*d*<sub>6</sub>):  $\delta$  71.08, 75.21, 90.90, 91.67, 92.99, 96.49, 107.56. IR (Nujol, KBr): 1595 (m), 1519 (m), 897 (w), 794 (w), 756 (m), 691 (m) cm<sup>-1</sup>. Anal. Calcd for C<sub>17</sub>H<sub>13</sub>Tl: C, 48.42; H, 3.10. Found: C, 48.50; H, 3.15.

(22) Shriver, D. F.; Dredzon, M. A. *The Manipulation of Air-Sensitive Compounds*, 2nd ed.; Wiley-Interscience: New York, 1986.

(23) (a) Kugel, M. *Liebigs Ann. Chem.* **1898**, 299, 50. (b) Drake, N. L.; Adams, J. R., Jr. *J. Am. Chem. Soc.* **1939**, 61, 1326.

(24) Ukay, T.; Kawazawa, H.; Ishii, Y.; Bonnett, J. J.; Ibers, J. A. *J. Organomet. Chem.* **1974**, 65, 253.

(25) Tate, D. P.; Knipple, W. R.; Augl, J. M. *Inorg. Chem.* **1962**, 1, 433.

(26) Coulson, D. R. *Inorg. Synth.* **1972**, 13, 121.

(27) Lorberth, J. *J. Organomet. Chem.* **1969**, 16, 327.

(28) Takahashi, S.; Kuroyama, Y.; Sonogashira, K.; Hagihara, N. *Synthesis* **1980**, 627.

(29) Jones, K.; Lappert, M. F. *J. Chem. Soc.* **1965**, 1944.

(30) Winkle, M. R.; Lansinger, J. M.; Ronald, R. C. *J. Chem. Soc., Chem. Commun.* **1980**, 87.

(19) Grushin, V. V.; Alper, H. *Chem. Rev.* **1994**, 94, 1047.

(20) Negishi, E.; Takahashi, T.; Baba, S.; Van Horn, D. E.; Okukado, N. *J. Am. Chem. Soc.* **1987**, 109, 2393.

(21) (a) Stang, P. J.; Kowalski, M. H. *J. Am. Chem. Soc.* **1989**, 111, 3356. (b) Portnoy, M.; Milstein, D. *Organometallics* **1993**, 12, 1655.

( $\eta^5$ -1-Ph<sub>2</sub>P-2,4-Ph<sub>2</sub>C<sub>5</sub>H<sub>2</sub>)(CO)<sub>3</sub>MoI (**12**). Compound **7** (9.77 g, 39.16 mmol) was dissolved in THF (60 mL) and then treated with 8.38 g (7.04 mL, 37.98 mmol) of chlorodiphenylphosphine. A white precipitate of thallium chloride was formed while the stirring was continued for 1 h. The mixture was then filtered, and the residue on the filter was washed three times with 20 mL portions of THF. BuLi (1.6 M solution in hexanes) (23.7 mL, 37.98 mmol) was then added to the filtrate, forming a pale orange solution of **9**. After 15 min, 11.51 g (37.98 mmol) of (CH<sub>3</sub>CN)<sub>3</sub>Mo(CO)<sub>3</sub> was added as solid. After overnight stirring, an intense orange solution was formed, and following a 1 h reflux and cooling at room temperature, 10.70 g (37.98 mmol) of solid 1,2-diiodoethane was added. A deep red solution was formed. After 2 h of stirring, approximately 20 g of Celite was added, and the solvent was removed under reduced pressure. The resulting residue was placed on a silica column (50 cm × 5 cm). Elution with hexane/dichloromethane (7/3) produced first a little yellow band, which was discarded, and then a second red band, which was collected. The latter, after removal of the solvent under vacuum left 26.63 g (98%) of **12** as red solid. The compound can be further purified by recrystallization from THF/pentane (vapor diffusion) at room temperature, forming the stoichiometrically bound THF complex **12**·THF; mp dec above 100 °C.

Anal. Calcd for C<sub>36</sub>H<sub>30</sub>O<sub>4</sub>IMoP: C, 55.4; H, 3.87. Found: C, 55.47; H, 3.77.

( $\eta^5$ -1-Ph<sub>2</sub>P-2,4-Ph<sub>2</sub>C<sub>5</sub>H<sub>2</sub>)(CO)<sub>3</sub>WI (**13**). This compound was prepared as described for **12**, by reacting 7.21 g (18.4 mmol) of (CH<sub>3</sub>CN)<sub>3</sub>W(CO)<sub>3</sub> and an equimolar amount of **9** to form **11** and subsequent treatment with 5.18 g (18.4 mmol) of 1,2-diiodoethane. The crude mixture was adsorbed on Celite and chromatographed on silica gel, using a gradient elution with a mixture of hexane/dichloromethane, and 11.57 g (79%) of product was recovered as red solid. Recrystallization from THF/pentane (vapor diffusion) at room temperature formed the stoichiometrically bound THF complex **13**·THF; mp 122–124 °C.

Anal. Calcd for C<sub>36</sub>H<sub>30</sub>O<sub>4</sub>IPW: C, 49.79; H, 3.48. Found: C, 49.66; H, 3.47.

( $\eta^5$ -1-Ph<sub>2</sub>P-2,4-Ph<sub>2</sub>C<sub>5</sub>H<sub>2</sub>)(CO)<sub>3</sub>MoPd(PPh<sub>3</sub>)I (**16**). A 100 mL Schlenk flask was loaded with 1.25 g (1.60 mmol) of **12**·THF, 1.21 g (2.11 mmol) of bis(dibenzylideneacetone)palladium, and 0.55 g (2.11 mmol) of triphenylphosphine. Following three cycles of evacuation/nitrogen filling, 20 mL of THF was added to the flask, causing the formation of a dark slurry, which only after several minutes of vigorous stirring turned to a deep red solution. After 1 h, approximately 20 g of Celite was added to the reaction mixture, and the solvent was removed under vacuum. The resulting residue was placed on a silica column (45 cm × 3 cm). Elution with hexane/dichloromethane (6/4) produced a rapidly moving pale yellow band, which was discarded. Elution was continued with a hexane/dichloromethane (4/6) mixture, and a red band developed, which was concentrated under vacuum and added to 50 mL of THF before being evaporated to complete dryness. In this way, 1.69 g (92%) of the THF bound complex **16**·THF was isolated as red solid. An analytical sample was obtained by recrystallization from THF/pentane (vapor diffusion) at room temperature; mp dec above 186 °C.

Anal. Calcd for C<sub>54</sub>H<sub>45</sub>O<sub>4</sub>MoIP<sub>2</sub>Pd: C, 56.44; H, 3.95. Found: C, 56.33; H, 3.46.

( $\eta^5$ -1-Ph<sub>2</sub>P-2,4-Ph<sub>2</sub>C<sub>5</sub>H<sub>2</sub>)(CO)<sub>3</sub>WPd(PPh<sub>3</sub>)I (**17**). This compound was prepared from 2.89 g (3.33 mmol) of **13**·THF, 2.50 g (4.35 mmol) of bis(dibenzylideneacetone)palladium, and 1.16 g (4.44 mmol) of triphenylphosphine in 50 mL of THF solvent as described for **16**. The crude mixture was adsorbed on Celite and chromatographed on silica column (5 cm × 55 cm). Elution with a hexane/dichloromethane (4/6) mixture produced a red band that, upon concentration, addition of THF (50 mL), and evaporation to dryness, afforded 3.34 g (81%) of **17**·THF as red solid. An analytical sample was obtained by recrystal-

lization from THF/pentane (vapor diffusion) at room temperature; mp dec above 204 °C.

Anal. Calcd for C<sub>54</sub>H<sub>45</sub>O<sub>4</sub>IP<sub>2</sub>PdW: C, 52.43; H, 3.67. Found: C, 52.58; H, 3.30.

**Preparation of Bu<sub>3</sub>SnC≡C(C<sub>6</sub>H<sub>4</sub>)p-NO<sub>2</sub> (**18**).** A mixture of 7.26 g (20.06 mmol) of (diethylamino)tributylstannane and 2.46 g (16.72 mmol) of (*p*-nitrophenyl)acetylene was stirred at room temperature for 3 h. Following removal under vacuum of the diethylamine formed during the reaction, pure product (5.68 g, 78%) was isolated by Kugelrohr distillation at 200 °C/10<sup>-2</sup> mm Hg.

<sup>1</sup>H NMR (CDCl<sub>3</sub>): δ 0.90 (t, 9H, *J* = 7.5 Hz, CH<sub>3</sub>CH<sub>2</sub>CH<sub>2</sub>-CH<sub>2</sub>Sn), 1.06 (t, 6H, *J* = 7.5 Hz, CH<sub>3</sub>CH<sub>2</sub>CH<sub>2</sub>CH<sub>2</sub>Sn), 1.33 (p, 6H, *J* = 7.5 Hz, CH<sub>3</sub>CH<sub>2</sub>CH<sub>2</sub>CH<sub>2</sub>Sn), 1.58 (ses, 6H, *J* = 7.5 Hz, CH<sub>3</sub>CH<sub>2</sub>CH<sub>2</sub>CH<sub>2</sub>Sn), 7.53 (d, 2H, *J* = 8.9 Hz, *o*-Ph), 8.12 (d, 2H, *J* = 8.9 Hz, *m*-Ph). <sup>13</sup>C NMR (CDCl<sub>3</sub>): δ 11.23, 13.65, 26.93, 28.85 (CH<sub>3</sub>CH<sub>2</sub>CH<sub>2</sub>CH<sub>2</sub>Sn), 101.36, 107.81 (-C≡C-), 123.43, 130.87, 132.53, 146.62 (Ph). IR (neat, KBr): 2956–2881 (br), 2447 (w), 1923 (w), 1794 (w), 1736 (w), 1678 (w), 1592 (s), 1517 (s), 1488 (m), 1460 (s), 1419 (w), 1337 (m), 1344 (s) cm<sup>-1</sup>. MS: *m/z* 380 (M<sup>+</sup> – Bu), 324 (M<sup>+</sup> – 2Bu), 266 (M<sup>+</sup> – 3Bu). The oily nature of the product does not allow elemental analyses to be accurately obtained.

( $\eta^5$ -1-Ph<sub>2</sub>P-2,4-Ph<sub>2</sub>C<sub>5</sub>H<sub>2</sub>)(CO)<sub>3</sub>MoPd(PPh<sub>3</sub>)C≡C(C<sub>6</sub>H<sub>4</sub>)p-NO<sub>2</sub> (**19**). A 100 mL Schlenk flask was loaded with 2.54 g (2.21 mmol) of **16**·THF and then evacuated/nitrogen filled three times. With the addition of 100 mL of DMF, a bright red solution was obtained. Following dropwise addition of 4-nitro-1-[2-(tributyltin)ethynyl]benzene (1.73 g, 3.97 mmol), the color changed to brown-orange, and the mixture was stirred for 1 h. The contents of the flask were then transferred to a separatory funnel, diluted with 100 mL of THF, and extracted with 6 × 100 mL portions of brine. The organic phase was then dried over magnesium sulfate, filtered, and concentrated. Pentane was then added until the solution became cloudy; the flask was stored in a freezer (-28 °C) overnight, producing an orange precipitate. The mother liquor was decanted and the product washed with pentane and dried under high vacuum, yielding 2.41 g (86%) of **19**·THF as a dark orange solid. An analytical sample was obtained upon recrystallization from THF/pentane (vapor diffusion) at room temperature; mp dec above 160 °C.

Anal. Calcd for C<sub>62</sub>H<sub>49</sub>O<sub>6</sub>MoNP<sub>2</sub>Pd: C, 63.74; H, 4.23. Found: C, 63.89; H, 4.5.

( $\eta^5$ -(1-Ph<sub>2</sub>P-2,4-Ph<sub>2</sub>)C<sub>5</sub>H<sub>2</sub>)(CO)<sub>3</sub>WPd(PPh<sub>3</sub>)C≡C(C<sub>6</sub>H<sub>4</sub>)p-NO<sub>2</sub> (**20**). This compound was prepared as described for **19** by reacting 2.0 g (1.61 mmol) of **17**·THF and 1.7 mL (1.26 g, 2.89 mmol) of 4-nitro-1-[2-(tributyltin)ethynyl]benzene in 80 mL of DMF as solvent. Following cold (-28 °C) precipitation with pentane from a concentrated THF solution, 1.70 g (90%) of the product was recovered as a dark solid. An analytical sample was obtained by recrystallization from THF/pentane (vapor diffusion) at room temperature; mp dec above 90 °C.

Anal. Calcd for C<sub>62</sub>H<sub>49</sub>O<sub>6</sub>NP<sub>2</sub>PdW: C, 59.28; H, 3.93. Found: C, 60.03; H, 4.02.

**X-ray Data Collection, Structure Determination, and Refinement for Complexes 13 and 17.** Red-purple crystals of **13** and red-orange crystals of **17** were grown at room temperature by vapor diffusion of pentane into the respective concentrated solution of the compound in THF. Both crystals were mounted on a Philips PW1100 single-crystal diffractometer; the symmetry and appropriate unit cell parameters were refined from least-squares calculations using the angular values of computer-centered reflections. Details are summarized in Table 3. Unfortunately, both crystals decomposed during the data collection procedures, resulting in low-quality experimental data. The corrections for the Lorentz and polarization effects and for the intensity decay were performed during the data reduction procedure.<sup>31</sup> The data of **13** were corrected for absorption with the  $\psi$  scan method,<sup>32</sup> and that

of Walker and Stuart<sup>33</sup> with the DIFABS<sup>34</sup> program was used to correct those of complex **17**. The structures were solved by direct methods,<sup>35</sup> and the refinement procedures were performed by full-matrix least-squares techniques with SHELX93.<sup>36</sup> The anisotropic thermal parameter of heavy atoms (the disordered atoms were kept isotropic) was used for complex **13**, while in complex **17**, all atoms were isotropic but tungsten, palladium, iodine, and phosphorus. Most of the H atoms of complex **13** were found in a  $\Delta F$  map, and the remaining H atoms were put in their calculated positions and all refined isotropically. In complex **17**, the hydrogens were fixed with

(31) Belletti, D. *A new hardware and software system for controlling the Philips PW1100 single crystal diffractometer with a personal computer*; Internal Report 1/94; Centro di Studio per la Strutturistica Diffrattometrica del C.N.R., Parma, Italy, 1994.

(32) North, A. C. T.; Phillips, D. C.; Matthews, F. S. *Acta Crystallogr.* **1968**, *A24*, 351.

(33) Walker, N.; Stuart, D. *Acta Crystallogr.* **1983**, *A39*, 158.

(34) Gluzinski, P. *XRAY, Set of programs for X-ray structural calculations*; Polish Academy of Sciences, Warszawa, Poland, 1989.

(35) Altomare, A.; Cascarano, G.; Giacovazzo, C.; Guagliardi, A.; Burla, M. C.; Polidori, C.; Camalli, M. *J. Appl. Crystallogr.* **1994**, *27*, 435.

(36) Sheldrick, G. M. *SHELX93. Program for the Refinement of Crystal Structures*; University of Göttingen, Germany, 1993.

idealized C–H = 0.80 Å. In both complexes, the solvent atoms were refined isotropically.

Some THF solvation was also present in both complexes. In complex **17**, the THF molecule was found with one carbon atom disordered in two different positions, while the exact disorder situation present in **13** could not be determined, and the molecule was found to be statistically distributed over many positions. Some constraints were applied to distances within the THF molecules. The H atoms associated with the disordered THF molecules were ignored. All calculations were performed on a DELL 486 personal computer with the Crys-ruler package.<sup>37</sup>

**Supporting Information Available:** Tables of crystallographic parameters, positional and thermal parameters, and complete interatomic distances and angles for complexes **13** and **17** and figures containing <sup>1</sup>H and <sup>31</sup>P NMR spectra (16 pages). Ordering information is given on any current mast-head page.

OM9601965

(37) Rizzoli, C.; Sangermano, V.; Calestani, G.; Andreotti, G. D. *J. Appl. Crystallogr.* **1987**, *20*, 436.